nanomaterials

MDPI

Article

Photocatalytic Semi-Hydrogenation of Alkynes: A Game of Kinetics, Selectivity and Critical Timing

Melissa Cely-Pinto, Bowen Wang and Juan C. Scaiano *

Department of Chemistry and Biomolecular Sciences, University of Ottawa, Ottawa, ON K1N 6N5, Canada; mcely097@uottawa.ca (M.C.-P.); bowenwanguv@gmail.com (B.W.)
* Correspondence: jscaiano@uottawa.ca

Abstract: The semi-hydrogenation reaction of alkynes is important in the fine chemicals and pharmaceutical industries, and it is thus important to find catalytic processes that will drive the reaction efficiently and at a low cost. The real challenge is to drive the alkyne-to-alkene reaction while avoiding over-hydrogenation to the saturated alkane moiety. The problem is more difficult when dealing with aromatic substitution at the alkyne center. Simple photocatalysts based on Palladium tend to proceed to the alkane, and stopping at the alkene with good selectivity requires very precise timing with basically no timing tolerance. We report here that the goal of high conversion with high selectivity could be achieved with TiO_2-supported copper (Cu@TiO_2), although with slower kinetics than for Pd@TiO_2. A novel bimetallic catalyst, namely, CuPd@TiO_2 (0.8% Cu and 0.05% Pd), with methanol as the hydrogen source could improve the kinetics by 50% with respect to Cu@TiO_2, while achieving selectivities over 95% and with exceptional timing tolerance. Further, the low Palladium content minimizes its use, as Palladium is regarded as an element at risk of depletion.

Keywords: photochemistry; heterogeneous catalysis; semi-hydrogenation; supported catalysts

Citation: Cely-Pinto, M.; Wang, B.; Scaiano, J.C. Photocatalytic Semi-Hydrogenation of Alkynes: A Game of Kinetics, Selectivity and Critical Timing. *Nanomaterials* **2023**, *13*, 2390. https://doi.org/10.3390/nano13172390

Academic Editors: Vincenzo Vaiano, Songlin Zhang and Zaicheng Sun

Received: 22 July 2023
Revised: 12 August 2023
Accepted: 18 August 2023
Published: 22 August 2023

1. Introduction

The semi-hydrogenation of alkynes to alkenes is one of the most important reactions in several industrial processes. Among the different hydrogenation reactions, the semi-hydrogenation of alkynes to alkenes is particularly challenging and important to the manufacture of bulk and fine chemicals. These reactions are commonly performed over supported Pd catalysts, which can be modified by the addition of different metals, including silver [1], or even using CO, which can act as a reversible poison [2,3]. For example, reports show that the semi-hydrogenation of phenylacetylene was performed using Pd nanoparticles in the forms of dispersed colloids [4] and supported systems [5,6]. The latter is more commercially attractive for industrial applications given their better handling properties, including post-reaction separation, and therefore, the development of heterogeneous catalysts with interesting compositions, high selectivity and catalytic efficiency will contribute to sustainable chemistry [7]. Different approaches have been explored, such as the one disclosed by Soberanas et al. [8], who synthesized solid-supported Pd-$(CaCO_3)_n$ clusters, showing a high catalytic activity for the semi-hydrogenation of internal alkynes compared with terminal alkynes, wherein, for example, internal aliphatic alkynes reacted faster with the catalyst than the aromatic ones. On the other hand, Wang et al. [9] proposed Pd-Se nanocrystals to enable the semi-hydrogenation of phenylacetylene to styrene, demonstrating the σ-π associative adsorption of the C≡C bond but suppressing the hydrogenation of C=C bond, which results in high selectivity. Zheng et al. [10] also worked with Pd, but in their case, they demonstrated that alloyed Pd-Pb on precipitated calcium carbonate (PCC) supports could be an upgraded version of the Lindlar catalyst that provides promising results for the semi-hydrogenation of phenylacetylene to styrene. Further, Lv et al. [11] developed a novel alumina-supported Pd catalyst for the selective

hydrogenation of phenylacetylene and less production of the byproduct ethylbenzene given the good dispersion of Pd and strong metal-support interaction capable of creating more active sites for hydrogenation and facilitating the desorption of the alkene.

However, even though different investigations have focused on increasing the selectivity of alkenes using different materials, the conversion of alkynes to alkanes is a straightforward process and can be performed quite efficiently if moieties other than the target alkyne are not affected in the process. Therefore, heterogeneous photocatalysts based on palladium over TiO_2 could be an alternative to the disclosed ones since they show excellent performance and the control over the light source might help during these processes. Different alternatives directed toward depositing metals over TiO_2 have also been explored as an effective approach to different materials in semi-hydrogenation reactions given its photon harvesting capacity and the increased charge separation that helps improve the semiconductor photocatalyst activity [12]. For example, such is the case for TiO_2 decorated with palladium nanoparticles (Pd@TiO_2). Some catalysts, like Pd@TiO_2, are excellent, and while the rate of first step k_1 tends to be faster than k_2, in reality, it is very difficult to stop at the critical point in time to achieve high selectivity. This is conceptually illustrated in Figure S1, where even if k_1 is 10 times faster than k_2 (panel B), only about 70% selectivity and about 70% alkene yield are obtained at 99% conversion. In contrast, when k_2 is 100 times slower than k_1 (panel C), the selectivity and yield are about 97% at 99% conversion. In other words, an alkene-selective catalyst must show very slow hydrogenation of alkenes while having an acceptable rate constant for alkyne hydrogenation.

Figure S1 is based on a very simple kinetic simulation, where the total time is equal to five lifetimes for the reagent decay according to first-order kinetics, reducing its concentration approximately 150 times. Heterogenous catalysis may not follow a simple kinetic model, but in any event, Figure S1 serves to illustrate the point. The expression "critical timing" used in the title relates to cases where it is possible to achieve reasonable selectivity in very fast reactions only if the reaction is stopped at a very precise time, while letting the reaction go for a bit longer (e.g., 20% longer) totally destroys the selectivity. The reality of the organic chemistry laboratory is that reaction times must be somewhat forgiving, as reaction times are measured in hours or overnight and rarely on continuous real-time monitoring of the reaction mixture composition.

Based on the above, semi-hydrogenation of alkynes can be a challenging process, as one would like to combine reasonable activity with high selectivity, such as illustrated in Scheme 1 for the case of 1-phenyl-1-propyne.

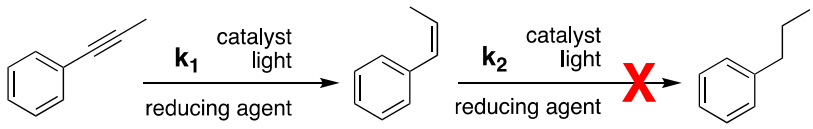

Scheme 1. Reaction path for semi-hydrogenation of 1-phenyl-1-propyne (PhP) using a photocatalyst. In an ideal situation $k_2 << k_1$.

On the other hand, other than Pd, different metals have been used in these reactions, for example, Cu on TiO_2 (Cu@TiO_2) showed sharp chemoselectivity when hydrogenating internal alkynes to alkenes without being further hydrogenated to alkanes [13]. However, according to Imai et al., when performing photocatalytic semi-hydrogenation of alkynes with Cu-Pd on TiO_2 (CuPd@TiO_2), the reaction works very well with aliphatic systems, but, for example, for 1-phenyl-acetylene in 2-propanol, the selectivity is reduced to 66% due to ongoing hydrogenation to ethylbenzene [14].

In this sense, the time of the reaction might be improved using a combination of two different elements. Additionally, beyond the hydrogenation kinetics on the surface of the catalyst, it is important to consider that selectivity is also controlled by the adsorption strength and the configuration of the reactants and intermediates on the surface of catalysts [15], and thus, these are parameters to consider when performing these reactions. Consequently, the ideal catalyst should prevent the over-hydrogenation of the formed

alkene while keeping acceptable reaction rates, selectivity and reactivity of the catalysts in these reactions.

Here, we compared catalysts based on Pd or Cu on TiO_2 (Pd@TiO_2 and Cu@TiO_2), as well as the mixture of both metals on TiO_2 (CuPd@TiO_2), with the last one prepared via galvanic exchange. We examined several alkynes, but frequently concentrated our detailed studies on 1-phenyl-1-propyne. All measurements included a detailed time profile showing the evolution of the reaction, avoiding end-point studies where conversions and selectivity measurements can reflect a poor choice of reaction times or irradiance values. The solvents and hydrogen donors were ethanol (EtOH) and methanol (MeOH) and the reactions were driven using UVA irradiation, which is a spectral region largely absorbed by TiO_2.

2. Results and Discussion

We tested three different catalysts and several alkynes. For selected combinations, we also examined the adsorption of the alkynes on the different materials, something that earlier work showed to be very important [15]. Finally, we looked at the catalytic properties of the materials, and in all cases, we examined the time dependence in detail. As Figure S1 illustrates, both the conversion and selectivity were critically dependent on time, and thus, end-point analysis was not particularly informative.

2.1. Catalyst Synthesis

Pd@TiO_2: Based on a reported synthesis [16–18]. Approximately 15 mg of metal precursor salt ($PdCl_2$) was mixed with TiO_2 (~500 mg) in 150 mL of Milli-Q water and sonicated for 20 min. The slurry was irradiated in a Luzchem photoreactor equipped with 14 UVA bulbs for 24 h with vigorous stirring in a crystallizing Pyrex® dish with a Pyrex® cover. The slurry was centrifuged and washed with Milli-Q water four times to remove unreacted metal precursor salt and dried overnight in a desiccator under vacuum. The obtained powder had a dark grey color.

Cu@TiO_2: Based on a reported synthesis [19]. A total of 33 mg of $CuCl_2{\cdot}2H_2O$ were mixed with TiO_2 (~500 mg) and 80 mg of Irgacure-2959 in 130 mL of Milli-Q water and purged with argon for 15 min. After this, the slurry was irradiated in a Luzchem photoreactor equipped with 14 UVA bulbs for 24 h with vigorous stirring. The slurry was filtered and washed with Milli-Q water at least seven times to remove unreacted metal precursor salt and dried overnight in a desiccator under vacuum. The powder had an intense beige color with green tones.

CuPd@TiO_2: The catalyst was obtained via galvanic replacement synthesis, which relies on the spontaneous redox reaction between the atoms of a substrate (Cu@TiO_2 previously synthesized) and the salt precursor ($Pd(acac)_2$ in this case) of another metal. Specifically, 0.28 mg of $Pd(acac)_2$ was mixed with 20 mL of Milli-Q water and sonicated for 15 min. After completing this, 10 mL of the solution was taken and mixed with 50 mg of Cu@TiO_2. The slurry was purged with argon for 15 min and vigorously stirred overnight. The slurry was filtered and washed with Milli-Q water at least seven times and dried overnight in a desiccator under vacuum. The powder had a similar color to the one from Cu@TiO_2.

2.2. Characterization

PdNP morphologies were approximately spherical. Transmission electron microscopy (TEM) images and a histogram for PdNPs are displayed in Figure 1. Additionally, for Cu@TiO_2 and CuPd@TiO_2, scanning electron microscopy (SEM) and energy-dispersive X-ray spectroscopy (EDS) were used to determine the presence of Cu and Pd in the catalysts. The TEM image of Pd@TiO_2 nanoparticles in panel A of Figure 1 shows a mean particle size of 3.0 ± 0.2 nm. On the other hand, according to EDS results of panels B and C of Figure 1, for Cu@TiO_2 and CuPd@TiO_2, the presence of Cu was identified for both catalysts, but it was not possible to identify the peak of Pd in CuPd@TiO_2 since the metal loading was too little (Table 1). X-ray photoelectron spectroscopy (XPS) analyses of Pd@TiO_2 and Cu@TiO_2

were conducted and published in previous publications, suggesting the presence of PdO with a small contribution of more reduced palladium species for $Pd@TiO_2$ [18] and satellite peaks of Cu (II) [20].

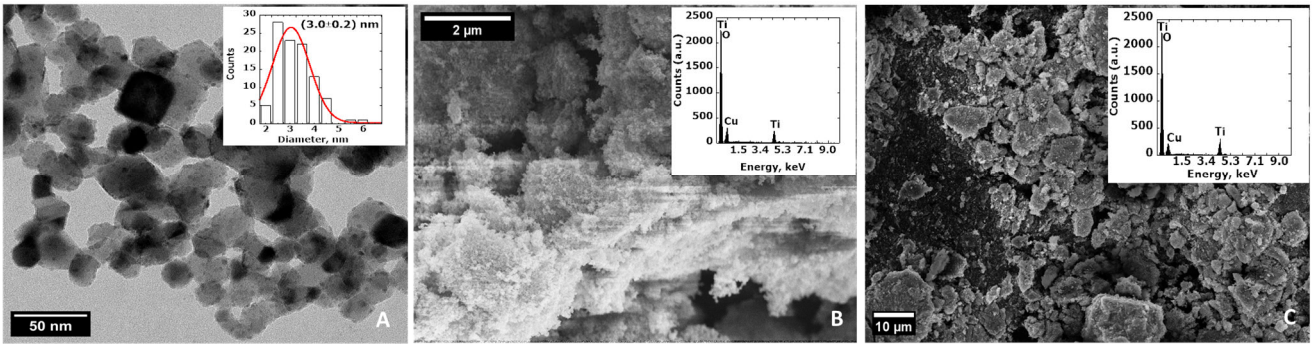

Figure 1. (**A**) TEM image of $Pd@TiO_2$ nanoparticles (histogram made with 100 particles (size bar is 50 nm). The mean particle size was 3.0 ± 0.2 nm. (**B**) SEM and EDS results for $Cu@TiO_2$. EDS results show the peaks for Ti, O and Cu, confirming the presence of Cu in the catalyst. (**C**) SEM and EDS results for $CuPd@TiO_2$. EDS results show the peaks for Ti, O and Cu, which corroborate the presence of Cu in the catalyst. However, it was not possible to identify the peak for Pd since the loading of this metal was too low (0.05% according to ICP).

Table 1. ICP-OES analysis of the catalysts before performing the adsorption experiments and semi-hydrogenation reactions.

Material	Metal Loading (%)
$Pd@TiO_2$	2.0 wt % Pd
$Cu@TiO_2$	0.9 wt % Cu
$CuPd@TiO_2$	0.8 wt % Cu and 0.05 wt % Pd

The metal loadings were determined using inductively coupled plasma optical emission spectroscopy (ICP-OES) analysis and are disclosed in Table 1.

2.3. Alkyne Adsorption on Selected Materials

Alkyne adsorption experiments are essential when looking at catalyzed reactions given that they might occur at the catalyst surface. In the present work, adsorption experiments were performed using two representative alkynes: 900 ppm solutions of phenylacetylene (PhA) and 1-phenyl-1-propyne (PhP) were stirred for 40 min in the presence of 10 mg of each material in EtOH. Preliminary experiments showed that 40 min was an adequate time to reach a plateau, that is, adsorption equilibration. A representative plot shown in Figure 2 and Table 2 summarizes the relevant data. Figure S4 also shows the results for PhP.

Table 2. Adsorption capacity of the catalysts when being in contact with PhA and PhP after 40 min of stirring.

Material	Phenylacetylene (PhA)	1-Phenyl-1-Propyne (PhP)
TiO_2	27%	13%
$Pd@TiO_2$ (2% Pd)	49%	37%
$Cu@TiO_2$ (0.9% Cu)	34%	19%
$CuPd@TiO_2$ (0.8% Cu and 0.05% Pd)	37%	20%

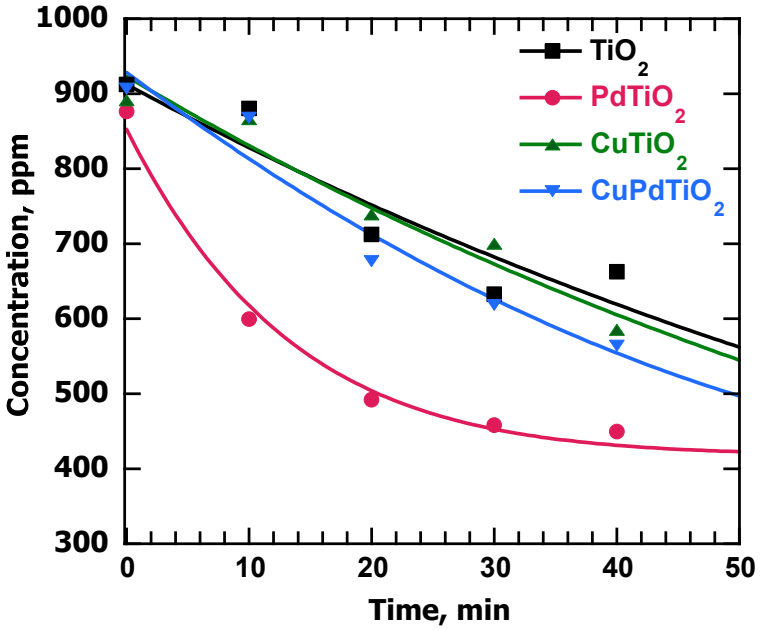

Figure 2. Adsorption experiments of PhA using the synthesized catalysts. Conditions: 10 mg catalyst; 1 mL of 900 ppm alkyne solution in ethanol. Stirring times: 0 min, 10 min, 20 min, 30 min and 40 min. Aliquots were taken at these times and filtered before using GC-MS to monitor the area under the peak of PhA at different times (3.70 min retention time identified using gas chromatography (GC), as shown in Figure S2, while Figure S3 shows the mass spectra of the alkynes). Calibration curves for every alkyne were necessary to determine the concentrations of the alkyne at the mentioned times using 3,5-Di-tert-butyltoluene as an external standard.

Examination of Table 2 shows that the metals played a key role in enhancing the adsorption properties of the TiO_2-supported systems. Note, for example, that in the case of PhP, 2% palladium content was enough to triple the amount of alkyne adsorbed when compared with TiO_2 itself. These data show that there was a significant number of sites over the Pd catalyst that strongly adsorbed the alkyne molecules. On the other hand, the effect of copper was also clear, but not as large as that of palladium. Additionally, the bimetallic catalyst exhibited similar adsorption to the one shown by Cu@TiO_2, even if the alkyne was internal. Also important, when preparing samples for catalysis studies, one must wait at least 30 min to ensure that the adsorption equilibrium is reached. Unfortunately, this information is rarely included in literature reports, but it is essential to understand different types of reactions, like semi-hydrogenation ones.

2.4. Semi-Hydrogenation of Alkynes with Single-Metal TiO_2 Catalysts

Scheme 2 shows the alkynes examined in this work. Among these, PhA and PhP were examined in more detail.

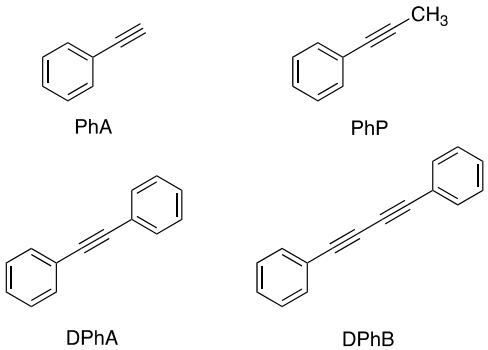

Scheme 2. Alkynes studied in this research.

All our studies involved irradiation with an LED UVA source centered at 370 nm (FWHM ~30 nm) with an adjustable irradiance (Figure S5). Under typical exposure conditions (4 cm from the emitter), the irradiance at 100% power was ~320 W/m^2, although when using Pd@TiO_2, most studies were performed at 25% power (~87 W/m^2) (Figure S6). Figure 3 shows the conversion against time for the four alkynes at 6 mM studied when the catalyst was Pd@TiO_2 and the hydrogen donor was EtOH.

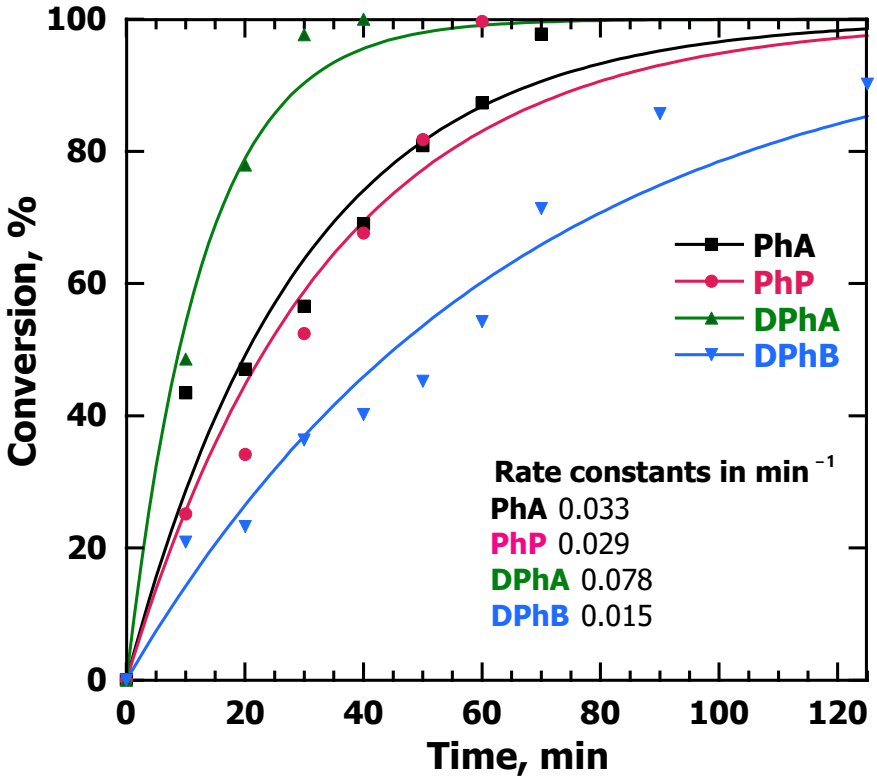

Figure 3. Conversion of alkynes after performing hydrogenation reactions using alkyne solutions in EtOH at a concentration of 6 mM under argon and irradiated with UVA light at 25% power and with 10 mg Pd@TiO_2 suspended in 8 mL. Under these conditions, the order of relative consumption rates changes, with DPhA showing the fastest consumption, while DPhB was the slowest one. Note that before these experiments, semi-hydrogenation reactions using 900 ppm as the main concentration for the alkynes were also performed. In this case, the molar concentrations were not the same for all alkynes (Figure S7), but rather the mass concentration was matched.

It was interesting to examine the performance of the alkynes with Pd@TiO_2 and EtOH as a solvent as a function of time. This is illustrated for PhP in Figure 4. The reaction was quite fast, reaching completion in under 80 min and a maximum yield of predominantly *cis* alkene at about 60 min when the remaining PhP was 4% and the selectivity toward alkenes was more than 90%, with about ~10% of 1-phenylpropane already formed at this point. Concerning the isomers formed in these reactions, in Figure S8 there is evidence that traces of the *trans*-isomer (retention time of 5.22 min in the GC chromatogram) were also formed, but the major product was the *cis*-compound (retention time of 4.90 min). Mechanistically, the reaction involves strong coordination between H (from the H source, in this case, the solvent) with Pd atoms in crystal lattices, and thus, the population of Pd sites was proposed to govern the hydrogenation events on the metal surface [21].

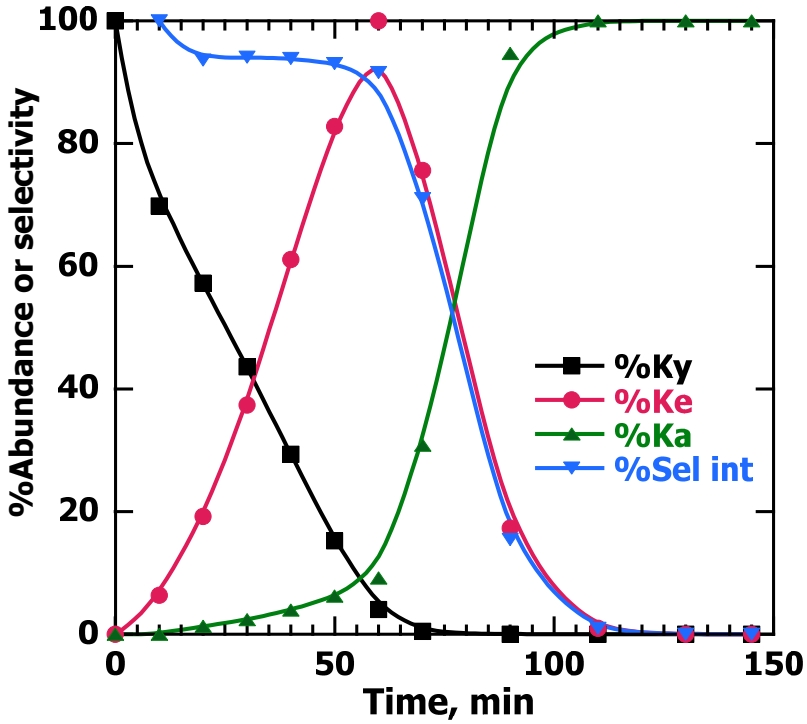

Figure 4. Abundance of the PhP (%Ky), along with alkenes (%Ke) and alkane (%Ka), and selectivity toward the alkenes (%Sel int) vs. time for 8 mL of a 6 mM solution in EtOH of PhP stirred with 10 mg of Pd@TiO_2. The reaction was performed in a Pyrex test tube with a rubber cap and irradiated with 25% UVA power under Ar. At 60 min, the abundance of the alkyne was more than 95% and the selectivity toward alkenes was 91%. Only 10 min longer made the selectivity 70% at 70 min.

Continuing with the analysis of Figure 4, it is worth highlighting that at times slightly longer than that required for alkyne consumption, the selectivity was reduced to 70% at 70 min and an additional 20 min reduced it to less than 20% (see "%Sel int" in Figure 4). This brings in the concept of critical timing, where in this case, it is not possible to achieve reasonable selectivity given that the reaction is very fast, and thus, stopping it at a very precise time might be difficult when working with Pd@TiO_2. It is possible to use Palladium catalysts for semi-hydrogenation, but the time at which the reaction must be stopped requires critical timing and an error of just a few minutes induces extensive over-hydrogenation to the alkane product.

The problem of critical timing occurs in spite of the fact that alkenes show less affinity for adsorption on the Pd@TiO_2 catalyst than alkynes. To verify this hypothesis, we tested the adsorption of DPhA vs. *cis* and *trans*-stilbene on Pd@TiO_2. Figure 5 shows these results obtained after stirring 1 mL of a 900 ppm solution for DPhA with 10 mg of Pd@TiO_2 for 40 min. A total of 41% adsorption was achieved since at 40 min, the concentration of the alkyne was reduced from 900 ppm to 520 ppm. Moreover, for the *cis* and *trans* isomers of stilbene, after 40 min, the adsorption on the surface catalyst was only 5% and 9%, respectively. Consequently, the adsorption of the alkyne on the catalyst surface was more efficient compared with the alkenes. For the semi-hydrogenation of alkynes, the literature suggests that alkynes adsorb more selectively on a metal surface, retarding alkene adsorption and hindering its hydrogenation to an alkane, as long as alkynes are still present in the reaction mixture [22]; these results might help to understand the semi-hydrogenation process.

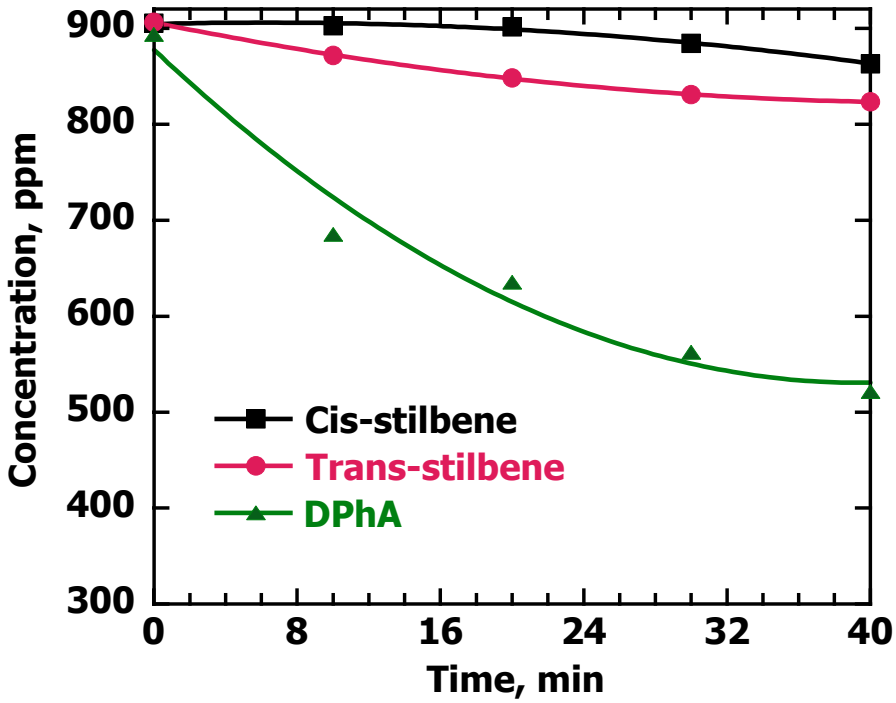

Figure 5. Adsorption of DPhA, cis and trans-stilbene on Pd@TiO_2. Solutions of the compounds in EtOH (900 ppm) and 10 mg of Pd@TiO_2 were stirred for 0, 10, 20, 30 and 40 min. Aliquots of the solution were taken at these times and filtered before analyzing them via GC-MS. The chromatograms provided via GC-MS were analyzed using calibration curves to determine the concentration of the compounds, where 3,5-di-tert-butyltoluene was used as an external standard.

The issue of critical timing illustrated in Figure 4 for PhP is not unique and similar problems are found for the other alkynes studied in this work (Figure S9) and summarized in Table 3. The loss of selectivity is rapid and large, which makes stopping the reaction at a critical time essential. Even 15 min will make the loss of selectivity quite large. For PhP, illustrated in Figure 4, a difference of 15 min with respect to t_{95} will reduce the selectivity to 59%, while stopping 15 min too soon will reduce the conversion and yield to 78%.

Table 3. Conversion and selectivity for the alkynes in Scheme 2 over time for 8 mL of 6 mM solutions in EtOH stirred with 10 mg of Pd@TiO_2 in Pyrex tubes and irradiated with 25% UVA power under Ar.

Item ↓/Molecule →	PhA	PhP	DPhA	DPhB
Time for 95% conversion, t_{95}	67 min	60 min	28 min	114 min
Selectivity at 95% conversion	95%	88%	79%	48%
Selectivity at 1.5 × t_{95}	52%	19%	11%	<1%
Selectivity at 2 × t_{95}	23%	<0.5%	<0.2%	~0

We also examined the effect of catalyst loading, illustrated in Figure S10 for PhP. We note that a reduction by a factor of five in the catalyst loading (2 mg rather than 10 mg of Pd@TiO_2) only reduced the rate of consumption by a factor of two. However, the issue of critical timing discussed in relation to Figure 4 and Table 3 remains unchanged. In general, small deviations from the critical time can cause large reductions in selectivity. Further, stopping early is not a solution either because the conversion curve is very steep and early stops lead to reduced conversion and yields.

The situation with Cu@TiO_2 as a catalyst was very different from that with Pd@TiO_2. The paragraphs and figures that follow elaborate on these differences. In brief, the copper catalyst was slower than palladium, but in terms of critical timing, it was very forgiving,

and over-hydrogenation was not a problem. In the qualitative context of Figure 1, one would estimate that $k_2 < 0.001\ k_1$. Initial experiments in this section were performed with 6 mM PhP and PhA in EtOH using 100% lamp power since when using 25%, the reaction can take days. Figure 6 shows the time evolution of the reaction over an extended period and with 100% lamp power. Even doubling the time required for 100% conversion, the yield of alkanes was minimal.

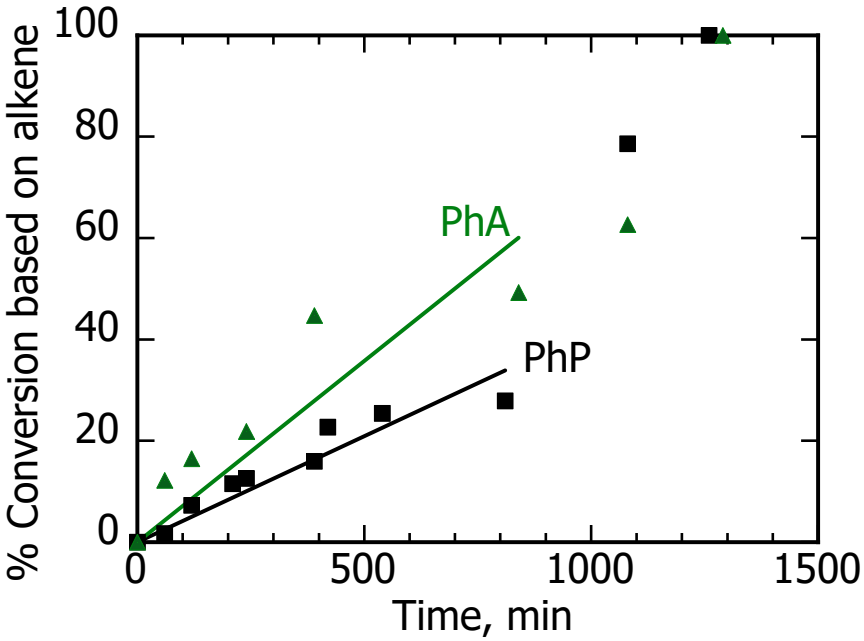

Figure 6. Conversion vs. time for PhA (green) and PhP (black). The samples consisted of 8 mL of 6 mM solutions in EtOH of the alkynes stirred with 10 mg of Cu@TiO_2 in different Pyrex tubes and irradiated with 25% UVA power under Ar. The fitting corresponds to low conversion (<50%) data and shows that PhA was 70% faster than PhP. The cis-alkene was essentially the only product with a selectivity exceeding 98% for the first 1000 min.

For Cu@TiO_2 in EtOH, there was no formation of 1-phenylpropane, even at longer times in comparison with the results obtained with Pd@TiO_2 (compare with Table 3). Copper showed a major improvement in the selectivity of the alkynes, even if the reaction was extended for 20 h. Accordingly, over-hydrogenation was not a problem, yet, the reaction time was around 10 times longer than that for Pd@TiO_2. Thus, the issue of longer reaction rates needs improvement.

In an attempt to improve the kinetics, we tried using a different solvent that may help to maintain the selectivity toward the alkenes and reduce reaction times [23]. According to this, MeOH was used as the hydrogen donor/solvent given its promising results in catalytic hydrogenation reactions. Hence, keeping the same conditions of the semi-hydrogenation reactions, Figure 7 shows the time profiles for PhP and PhA when performing the semi-hydrogenation reactions in EtOH and MeOH.

The results of Figure 7 show that MeOH, as both the hydrogen donor and solvent, increased the rates of reaction. These results show that the rate of alkyne-to-alkene reaction when using Cu@TiO_2 and MeOH could be improved while avoiding over-hydrogenation to the saturated alkane moiety. Control experiments were also performed and Figure S12 shows the results for the reaction of PhP in MeOH with TiO_2 itself, where after 540 min (9 h) of reaction, less than 5% of PhP was consumed and barely around ~1% of *cis*-1-phenyl-1-propene was produced. This confirms that decorating TiO_2 with a metal improved the photocatalytic activity of the material for these reactions.

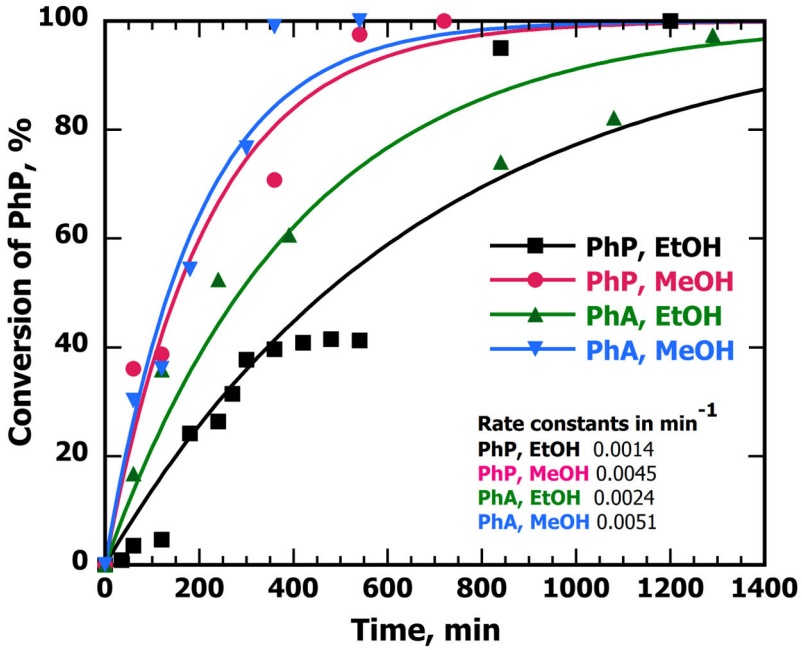

Figure 7. Conversion of PhA and PhP in MeOH and EtOH vs. time. A total of 8 mL of 6 mM solutions in MeOH and EtOH of the alkynes were stirred with 10 mg of $Cu@TiO_2$ in different Pyrex® containers and irradiated with 100% UVA power under Ar. The data were fit with an exponential forced fit to start at zero and level off at 100%; the curves are mostly presented to help the reader visualize data trends.

2.5. Semi-Hydrogenation of Alkynes with the Bimetallic CuPd@TiO$_2$ Catalyst

The motivation to test a bimetallic catalyst relates to the excellent selectivity of $Cu@TiO_2$ and the excellent kinetics of $Pd@TiO_2$. Based on previous results, we wondered whether light-initiated incorporation of palladium to the $Cu@TiO_2$ catalyst may help with the kinetics without significant loss of selectivity and without creating an important critical timing issue. With this in mind, we prepared $CuPd@TiO_2$ via galvanic replacement, with a loading of 0.8% copper and 0.05% palladium. The catalyst was tested in a MeOH suspension with solutions of 6 mM PhP in MeOH and two different catalyst loadings, namely, 10 mg and 5.4 mg, which are shown in Figure S11. The choice of MeOH reflects the observation of improved kinetics shown in Figure 7. In order to compare the different catalysts, we selected 6 mM of PhP and 10 mg of the catalyst under the conditions specified in the caption of Figure 8. Please note that the $CuPd@TiO_2$ catalyst was prepared from a sample of the same $Cu@TiO_2$ material used in the experiment.

Table 4. Comparison of catalyst performance under the conditions of Figure 8.

Catalyst	Alkyne Rate of Consumption (min^{-1})	Selectivity at 95% Alkyne Conversion	Selectivity at Twice the Time for 95% Conversion
$Cu@TiO_2$	0.19	>99%	84%
$CuPd@TiO_2$	0.29	>99%	97%
$Pd@TiO_2$	3.94	88%	<1%

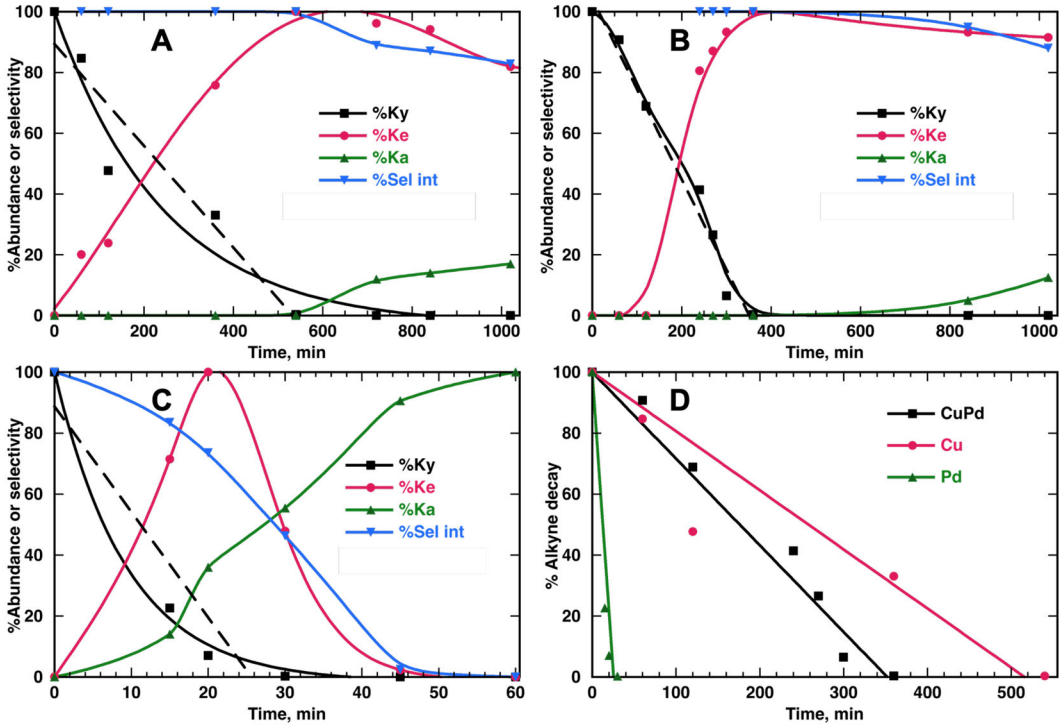

Figure 8. (**A**) Comparison of catalytic performance for 8 mL of 6 mM PhP solution in MeOH stirred with 10 mg of catalyst and irradiated with 25% UVA power under Ar for Cu@TiO_2, (**B**) CuPd@TiO_2 and (**C**) Pd@TiO_2. Panel (**D**) compares the different consumption slopes (100% to 5%) for the alkyne with the different catalysts. The kinetic data are also summarized in Table 4. Dashed lines fit the early linear data.

Table 4 shows that incorporating traces of Pd (see Table 1) was enough to increase the rate by 52% with respect to Cu@TiO_2, and it even remained much slower than Pd@TiO_2.

The observed performance of the bimetallic CuPd@TiO_2 catalyst was improved over previously reported catalysts, including the Lindlar Pd catalyst and other systems where, for example, the addition of organic ligands is needed to avoid over-hydrogenation of alkenes to alkane [24,25]. Along this line of thought and in agreement with previous reports based on Pd bimetallic catalysts [26,27], the possible absence of substantial Pd agglomeration results in weak adsorption toward alkene on the catalyst surface and high alkene selectivity. It is also remarkable that panel B in Figure 8 shows better long-term selectivity than panel A. Surprisingly, a small amount of Pd not only increased the rate of reaction but caused a selectivity improvement. Additionally, it is worth highlighting that the light source was essential for photocatalytic reactions like these. According to the results of Figure S13, when the reaction for PhP and 10 mg of CuPd@TiO_2 was performed without light, for at least 9 h, there was no consumption of the alkyne nor production of alkenes.

The mechanism by which palladium improves reactivity without a decrease in selectivity is probably similar to that for palladium on gold, where it is believed that hydrogen atoms generated on Pd leak into the second metal where the reaction takes place [28]. In this case, H atoms from the solvent, either EtOH or MeOH, generated on Pd would be transferred to the copper that controls the selectivity of the reaction, as depicted in Figure 9.

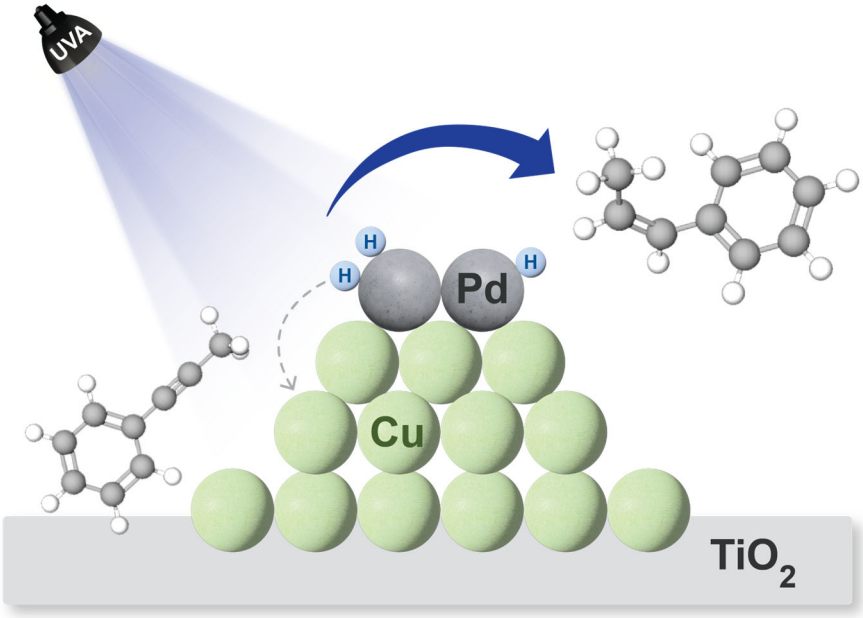

Figure 9. Plausible scenario to understand the activity shown by CuPd@TiO_2. Figure inspired by similar concepts in the literature [28].

Therefore, introducing Pd, which can rapidly speed up the reaction, on the Cu/TiO_2 catalyst, which has been shown to be much more chemoselective, helped to improve the selectivity toward alkenes in this photocatalytic reaction and the critical timing control was forgiving when reaction times were measured in hours or overnight.

3. Materials and Methods

3.1. Materials

Chemicals and materials were sourced from multiple suppliers for the experimental work. The initiator Irgacure-2959 was a gift from BASF, while the alkynes, solvents (spectrophotometric grade >99.8%), $PdCl_2$, $CuCl_2{\cdot}2H_2O$ and $Pd(acac)_2$ were purchased from Sigma Aldrich. TiO_2 P25 was purchased from Univar Canada. The MilliQ water was obtained via purification of deionized water using a Thermo Scientific™ Barnstead™ GenPure™ (Waltham, MA, USA)water purification system (conductivity 18 MΩ/cm).

3.2. Instruments

The photocatalytic performance of the catalysts at the bench scale was examined in Pyrex® test tubes. The reaction mixture was stirred and irradiated using a UVA Kessil lamp PR160-370 nm with a controllable LED at different powers (25% and 100%). The synthesis of the catalysts was performed by using a Luzchem photoreactor equipped with 14 UVA bulbs. Transmission electron microscope (TEM) images were acquired at the University of Ottawa's Materials Characterization Facility (MatChar) with a JEM2100F FETEM (JEOL, Tokyo, Japan) field emission transmission electron microscope. Particle sizes were determined with ImageJ analysis. Scanning electron microscopy (SEM, Zeiss, Jena, Germany) and energy-dispersive X-ray spectroscopy (EDS, Bruker, Milton, ON, Canada) images were acquired at the NanoFab Facility at the University of Ottawa with a Zeiss GeminiSEM 500 column using a Schottky thermal field emitter filament for imaging between 0.1 and 30 kV for sub-nanometer resolution imaging and with a Bruker EDS detector suitable for X-ray detection for spot identification of the composite. The metal loading of catalysts was determined using inductively coupled plasma emission spectrometry (ICP-OES) using an Agilent Vista Pro ICP Emission Spectrometer (Santa Clara, CA, USA). Characterization of the semi-hydrogenation reactions and their products was performed by using mass

spectrometry in an Agilent 6890-N Gas Chromatograph with an Agilent 5973 mass selective detector (Santa Clara, CA, USA).

3.3. Semi-Hydrogenation Reactions

The reactions were performed in 15 mL Pyrex® test tubes with a rubber cap. In a typical reaction, 8 mL of 900 ppm or 6 mM alkyne solution in EtOH was stirred with 10 mg of catalyst (Pd@TiO_2, Cu@TiO_2) and irradiated with a 25% or 100% UVA light source at 4 cm from the test tube. The reaction mixture was purged with argon. Similar preparations were also made using methanol as the solvent and using either the mentioned catalysts or CuPd@TiO_2. Aliquots were taken at regular intervals and filtered using syringe filters with a PTFE membrane in order to remove the catalyst before using an Agilent 6890-N Gas Chromatograph with an Agilent 5973 mass selective detector to monitor the reactions and identify the peaks of the reactants and products. Every time the aliquots were taken, purging the reaction with Ar was necessary in order to assure the inert environment. Calibration curves for every alkyne were necessary to determine the concentration of the alkyne at the mentioned times using 3,5-di-tert-butyltoluene as an external standard.

4. Conclusions

Semi-hydrogenations always present significant challenges, as the interplay of kinetics and selectivity determine the performance of the catalyst. The reality of the organic laboratory is that reactions are not stopped at exact times and reaction end points are frequently controlled by convenience, such as in the case of "overnight reactions". Reactions that can lose their yield or selectivity over short periods are simply impractical. Such is the case of Pd@TiO_2 as a catalyst, where critical timing is essential to preserve high yields and selectivity. In contrast, Cu@TiO_2 and CuPd@TiO_2 offer excellent selectivity without critical timing requirements. The latter was about 52% faster than Cu@TiO_2 and to our surprise, not only preserved the selectivity but also offered a small improvement (compare Figure 9 panels A and B). Thus, for alkyne semi-hydrogenation, we recommend CuPd@TiO_2 as a catalyst and methanol as the solvent. These results open the way to synthesizing highly active and selective catalysts inspired by the reality of timing control of semi-hydrogenation processes at the bench scale. However, future work should focus on further exploration to optimize even more the time of the reaction to complete the semi-hydrogenation process in less time but without losing great selectivity and still having control over the critical point between progressing from an alkene to an alkane.

Supplementary Materials: The following supporting information can be downloaded from https://www.mdpi.com/article/10.3390/nano13172390/s1: Figures S1–S13: GC-MS characterization, results for adsorption experiments of PhP at 900 ppm, spectral irradiance of the UVA source employed in the semi-hydrogenation reactions under different conditions, TEM images and the corresponding size histogram SEM/EDS analysis, and conversion of alkynes and selectivity toward alkenes at different conditions. Control experiments without light and with TiO_2 itself have been added to show the effect of the used metals.

Author Contributions: The concept for this research was proposed by J.C.S. All the experimental work was performed by M.C.-P. with help from B.W., who performed and interpreted the ICP studies. The preparation of the manuscript and interpretation of the results was a joint effort between the authors. All authors have read and agreed to the published version of the manuscript.

Funding: This research was funded by the Natural Sciences and Engineering Research Council of Canada, the Canada Foundation for Innovation and the Canada Research Chairs Program.

Data Availability Statement: Original data are available from the corresponding author upon reasonable request.

Acknowledgments: Rhiannon Hendley helped initially in the adsorption experiments of the alkynes on Pd@TiO_2.

Conflicts of Interest: The authors declare no conflict of interest.

References

1. Zea, H.; Lester, K.; Datye, A.K.; Rightor, E.; Gulotty, R.; Waterman, W.; Smith, M. The influence of Pd-Ag catalyst restructuring on the activation energy for ethylene hydrogenation in ethylene-acetylene mixtures. *Appl. Catal. A* **2005**, *282*, 237–245. [CrossRef]
2. Nikolaev, S.A.; Zanaveskin, L.N.; Smirnov, V.V.; Averyanov, V.A.; Zanaveskin, K.L. Catalytic hydrogenation of alkyne and alkadiene impurities from alkenes. Practical and theoretical aspects. *Russian Chem. Rev.* **2009**, *78*, 231–247. [CrossRef]
3. Borodziński, A.; Bond, G.C. Selective hydrogenation of ethyne in ethene-rich streams on palladium catalysts, Part 2: Steady-state kinetics and effects of palladium particle size, carbon monoxide, and promoters. *Catal. Rev. Sci. Eng.* **2008**, *50*, 379–469. [CrossRef]
4. Domínguez-Domínguez, S.; Berenguer-Murcia, Á.; Cazorla-Amorós, D.; Linares-Solano, Á. Semihydrogenation of phenylacetylene catalyzed by metallic nanoparticles containing noble metals. *J. Catal.* **2006**, *243*, 74–81. [CrossRef]
5. Domínguez-Domínguez, S.; Berenguer-Murcia, Á.; Pradhan, B.K.; Linares-Solano, Á.; Cazorla-Amorós, D. Semihydrogenation of phenylacetylene catalyzed by palladium nanoparticles supported on carbon materials. *J. Phys. Chem. C* **2008**, *112*, 3827–3834. [CrossRef]
6. Chaudharl, R.V.; Jaganathan, R.; Kolhe, D.S. Effect of Catalyst Activity Selectivity Hydrogenation of Phenylacetylene oveerr Pd/C Catalyst. *Ind. Eng. Chem. Prod. Res. Dev.* **1986**, *25*, 375–379. [CrossRef]
7. Song, S.; Li, K.; Pan, J.; Wang, F.; Li, J.; Feng, J.; Yao, S.; Ge, X.; Wang, X.; Zhang, H. Achieving the Trade-Off between Selectivity and Activity in Semihydrogenation of Alkynes by Fabrication of (Asymmetrical Pd@Ag Core)@(CeO_2 Shell) Nanocatalysts via Autoredox Reaction. *Adv. Mat.* **2017**, *29*, 1–6. [CrossRef]
8. Ballesteros-Soberanas, J.; Hernández-Garrido, J.C.; Cerón-Carrasco, J.P.; Leyva-Pérez, A. Selective semi-hydrogenation of internal alkynes catalyzed by Pd–CaCO3 clusters. *J. Catal.* **2022**, *408*, 43–55. [CrossRef]
9. Wang, M.; Liang, L.; Liu, X.; Sun, Q.; Guo, M.; Bai, S.; Xu, Y. Selective semi-hydrogenation of alkynes on palladium-selenium nanocrystals. *J. Catal.* **2023**, *418*, 247–255. [CrossRef]
10. Zheng, Y.; Gu, L.; Li, Y.; Ftouni, J.; Dutta Chowdhury, A. Revisiting the Semi-Hydrogenation of Phenylacetylene to Styrene over Palladium-Lead Alloyed Catalysts on Precipitated Calcium Carbonate Supports. *Catalysts* **2023**, *13*, 50. [CrossRef]
11. Lv, J.; Wang, D.; Guo, X.; Ding, W.; Yang, W. Selective hydrogenation of phenylacetylene over high-energy facets exposed nanotubular alumina supported palladium catalysts. *Catal. Commum.* **2023**, *181*, 106715. [CrossRef]
12. Huang, R.; Wu, J.; Zhang, M.; Liu, B.; Zheng, Z.; Luo, D. Strategies to enhance photocatalytic activity of graphite carbon nitride-based photocatalysts. *Mat. Des.* **2021**, *210*, 110040. [CrossRef]
13. Kominami, H.; Higa, M.; Nojima, T.; Ito, T.; Nakanishi, K.; Hashimoto, K.; Imamura, K. Copper-Modified Titanium Dioxide: A Simple Photocatalyst for the Chemoselective and Diastereoselective Hydrogenation of Alkynes to Alkenes under Additive-Free Conditions. *ChemCatChem* **2016**, *8*, 2019–2022. [CrossRef]
14. Imai, S.; Nakanishi, K.; Tanaka, A.; Kominami, H. Accelerated Semihydrogenation of Alkynes over a Copper/Palladium/Titanium (IV) Oxide Photocatalyst Free from Poison and H_2 Gas. *ChemCatChem* **2020**, *12*, 1609–1616. [CrossRef]
15. Zhao, X.; Zhou, L.; Zhang, W.; Hu, C.; Dai, L.; Ren, L.; Wu, B.; Fu, G.; Zheng, N. Thiol Treatment Creates Selective Palladium Catalysts for Semihydrogenation of Internal Alkynes. *Chem* **2018**, *4*, 1080–1091. [CrossRef]
16. Hainer, A.; Marina, N.; Rincon, S.; Costa, P.; Lanterna, A.E.; Scaiano, J.C. Highly electrophilic titania hole as a versatile and efficient photochemical free radical source. *J. Am. Chem. Soc.* **2019**, *141*, 4531–4535. [CrossRef]
17. Elhage, A.; Lanterna, A.E.; Scaiano, J.C. Tunable Photocatalytic Activity of Palladium-Decorated TiO2: Non Hydrogen -Mediated Hydrogenation or Isomerization of BenzylSubstituted Alkenes. *ACS Catal.* **2017**, *7*, 250–255. [CrossRef]
18. Elhage, A.; Lanterna, A.E.; Scaiano, J.C. Catalytic farming: Reaction rotation extends catalyst performance. *Chem. Sci.* **2019**, *10*, 1419–1425. [CrossRef]
19. Wang, B.; Lanterna, A.E.; Scaiano, J.C. Mechanistic Insights on the Semihydrogenation of Alkynes over Different Nanostructured Photocatalysts. *ACS Catal.* **2021**, *11*, 4230–4238. [CrossRef]
20. Wang, B.; Durantini, J.; Nie, J.; Lanterna, A.E.; Scaiano, J.C. Heterogeneous Photocatalytic Click Chemistry. *J. Am. Chem. Soc.* **2016**, *138*, 13127–13130. [CrossRef]
21. Fan, Q.; He, S.; Hao, L.; Liu, X.; Zhu, Y.; Xu, S.; Zhang, F. Photodeposited Pd Nanoparticles with Disordered Structure for Phenylacetylene Semihydrogenation. *Sci. Rep.* **2017**, *7*, 42172. [CrossRef] [PubMed]
22. Nikolaev, S.A.; Smirnov, V.V. Synergistic and size effects in selective hydrogenation of alkynes on gold nanocomposites. *Catal. Today* **2009**, *147*, S336–S341. [CrossRef]
23. Sklyaruk, J.; Zubar, V.; Borghs, J.C.; Rueping, M. Methanol as the Hydrogen Source in the Selective Transfer Hydrogenation of Alkynes Enabled by a Manganese Pincer Complex. *Org. Lett.* **2020**, *22*, 6067–6071. [CrossRef] [PubMed]
24. Kwon, S.G.; Krylova, G.; Sumer, A.; Schwartz, M.M.; Bunel, E.E.; Marshall, C.L.; Chattopadhyay, S.; Lee, B.; Jellinek, J.; Shevchenko, E.V. Capping Ligands as Selectivity Switchers in Hydrogenation Reactions. *Nano Lett.* **2012**, *12*, 5382–5388. [CrossRef] [PubMed]
25. Albani, D.; Shahrokhi, M.; Chen, Z.; Mitchell, S.; Hauert, R.; López, N.; Pérez-Ramírez, J. Selective ensembles in supported palladium sulfide nanoparticles for alkyne semi-hydrogenation. *Nat. Commum.* **2018**, *9*, 2634. [CrossRef]
26. Pei, G.X.; Liu, X.Y.; Yang, X.; Zhang, L.; Wang, A.; Li, L.; Wang, H.; Wang, X.; Zhang, T. Performance of Cu-Alloyed Pd Single-Atom Catalyst for Semihydrogenation of Acetylene under Simulated Front-End Conditions. *ACS Catal.* **2017**, *7*, 1491–1500. [CrossRef]

27. Da Silva, F.P.; Fiorio, J.L.; Gonçalves, R.V.; Teixeira-Neto, E.; Rossi, L.M. Synergic Effect of Copper and Palladium for Selective Hydrogenation of Alkynes. *Ind. Eng. Chem. Res.* **2018**, *57*, 16209–16216. [CrossRef]
28. Serna, P.; Concepción, P.; Corma, A. Design of highly active and chemoselective bimetallic gold–platinum hydrogenation catalysts through kinetic and isotopic studies. *J. Catal.* **2009**, *265*, 19–25. [CrossRef]